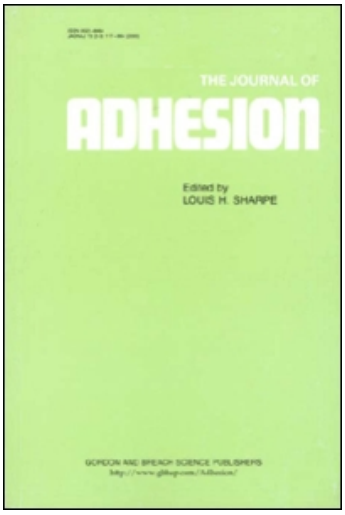

The Journal of Adhesion
Publication details, including instructions for authors and subscription information:
http://www.informaworld.com/smpp/title~content=t713453635

Particle Detachment from Rough Surfaces in Turbulent Flows

Mehdi Soltani[a]; Goodarz Ahmadi[a]
[a] Department of Mechanical and Aeronautical Engineering, Clarkson University, Potsdam, NY, USA

To cite this Article Soltani, Mehdi and Ahmadi, Goodarz(1995) 'Particle Detachment from Rough Surfaces in Turbulent Flows', The Journal of Adhesion, 51: 1, 105 — 123
To link to this Article: DOI: 10.1080/00218469508009992
URL: http://dx.doi.org/10.1080/00218469508009992

J. Adhesion, 1995, Vol. 51, pp. 105–123
Reprints available directly from the publisher
Photocopying permitted by license only

Particle Detachment from Rough Surfaces in Turbulent Flows*

MEHDI SOLTANI and GOODARZ AHMADI**

Department of Mechanical and Aeronautical Engineering, Clarkson University, Potsdam, NY 13699-5725, USA

(Received March 3, 1994; in final form July 8, 1994)

Two flow structure-based models for particle resuspension from rough surfaces in turbulent streams are developed. It is assumed that the real area of contact is determined by elastic deformation of asperities and the effect of topographic properties of surfaces are included. The JKR adhesion model is used to analyze the behaviour of individual asperities. The theories of rolling and sliding detachment are used and the flow-induced resuspension is studied. The effects of the near-wall coherent eddies, and turbulence urst/inrush motion are included in the model development. The critical shear velocities needed to detach different sized particles from rough surfaces under various conditions are evaluated and discussed. The model predictions are compared with the available experimental data and good agreement is obtained.

KEY WORDS adhesion; detachment; roughness; turbulent flow; resuspension.

INTRODUCTION

Flow-induced particle removal from real surfaces has attracted considerable attention due to numerous industrial applications. During the last few decades, many studies concerning particle detachment from surfaces were published. Extensive reviews of particle adhesion mechanisms were provided by Corn,[1] Zimon,[2] Krupp,[3] Visser,[4] Tabor,[5] Bowling,[6] and Ranade.[7]

The effect of contact deformation on adhesion was considered by Derjaguin.[8] The influence of surface energy and elastic deformation on adhesion force was analyzed by Johnson *et al.*[9] Their results led to what is now known as the JKR adhesion model. Works related to particle adhesion were reported by Derjaguin *et al.*[10] Muller *et al.*[11,12] Tsai *et al.*[13] and Rimai *et al.*[14]

A number of authors studied particle re-entrainment processes. Cleaver and Yates[15] developed a particle resuspension model based on the lift force arising from the turbulence bursts. Masironi and Fish[16] studied the particle re-entrainment and reported particle rolling movement on the surface. The mechanisms for resuspension of small particles were studied by Punjrath and Heldman[17] through a series of wind tunnel experiments. Extensive reviews of resuspension processes and the available

*Presented in part at the Seventeenth Annual Meeting of The Adhesion Society, Inc., in Orlando, Florida, U. S. A., February 21–23, 1994.

**Corresponding author.

models were provided by Healy,[18] Sehmel,[19] Smith *et al.*[20] Hinds[21] and Nicholson.[22] Soltani and Ahmadi[23] studied turbulence resuspension models based on sublayer and turbulence burst/inrush flows using the theories of rolling detachment and sliding removal. Wen and Kasper[24] proposed a kinetic model for particle resuspension.

Most earlier resuspension studies were almost exclusively concerned with smooth surfaces. Real surfaces, however, are rough and this causes the real area of contact to be extremely small compared with the nominal area. Greenwood and Williamson[25] presented a new theory of elastic contact, which was more closely related to real surfaces than earlier theories. They proposed that the contact deformation depends on the topography of the surface. Greenwood[26] described a surface model consisting of an assembly of similar idealized asperities. Greenwood and Tripp[27] improved the Hertz contact model by taking into account the effect of roughness. Fuller and Tabor[28] studied the effect of roughness on the adhesion of elastic solids. They found that relatively small surface roughnesses are sufficient to reduce the adhesion force significantly. Johnson[29] described the role of surface roughness in reducing particle adhesion. A dynamic model for the long term resuspension of small particles from smooth and rough surfaces in turbulent flow was developed by Reeks *et al.*[30] and Reeks and Hall.[31]Soltani and Ahmadi[32] studied the effect of surface roughness on particle removal mechanisms subject to substrate accelerations.

In this work, the effect of surface roughness on particle resuspension in turbulent flows is studied. Re-entrainment models based on sublayer and turbulence burst/inrush flows are developed. Each asperity is assumed to have an elastic deformation following the JKR adhesion theory. Near-wall flows are modeled as viscous stagnation point flows. The theory of critical moment and sliding detachment mechanisms are used in the model developments. The minimum critical shear velocities required to detach various size particles from rough surfaces under different conditions are evaluated. Comparison of the model predictions with the experimental data are also performed.

ADHESION MODEL

In this section, a brief summary of the JKR adhesion model used in this study is presented. According to the JKR model, the pull-off force F_{po} and the contact radius, a, of a spherical particle at the moment of detachment are given by

$$F_{po} = \tfrac{3}{4}\pi W_A d, \tag{1}$$

$$a = (F_{po} d/2K)^{1/3}, \tag{2}$$

where K is the composite Young's modulus given as

$$K = \frac{4}{3}\left[\frac{(1-\nu_1^2)}{E_1} + \frac{(1-\nu_2^2)}{E_2}\right]^{-1} \tag{3}$$

Here, d is the diameter of the spherical particle, W_A is the thermodynamic work of

adhesion, and v_i and E_i are, respectively, the Poisson's ratio, and the Young's modulus of material $i(i = 1$ or 2).

SURFACE ROUGHNESS MODEL

The analysis of Johnson *et al.*[9] of the contact of elastic spheres in the presence of adhesive forces is applied to the contact of individual asperities by Fuller and Tabor.[28] They postulated that all asperities have the same radius and that their heights vary randomly, following a Gaussian distribution. They also assumed that each asperity will be deformed elastically following the JKR theory. Soltani and Ahmadi[32] proposed an analytical expression for the force needed to detach the particle from rough surfaces. Accordingly, the total pull-off force for a rough surface is given as

$$F_M = \pi a^2 N f_{po} \exp[-0.6/(\Delta_c)^2], \tag{4}$$

where f_{po} is the maximum force which can be sustained by adhesion before separation of individual asperities, a is the contact radius, and N is the number of asperities per unit area. The nondimensional variable Δ_c is defined as

$$\Delta_c = \delta_c/\sigma, \tag{5}$$

where σ is the standard deviation of the height distribution, and δ_c is the maximum extension of the tip of an asperity above its undeformed height before the adhesion breaks. According to the JKR adhesion theory

$$\delta_c = \left[\frac{f_{po}^2}{3K^2\beta}\right]^{1/3}, \tag{6}$$

where β is the radius of an asperity. Note that $\Delta_c^{-1} = \sigma/\delta_c$ is an appropriate measure of surface roughness.

The contact radius of a spherical particle attached to a rough surface is not known. Here the contact radius is estimated based on the JKR theory with an adjusted pull-off load. *i.e.*,

$$a = (F_M d/2K)^{1/3} \tag{7}$$

The topographical data for real surfaces presented by Greenwood and Williamson[25] showed that for real surfaces the quantities, σ, β and N are related by

$$\sigma\beta N \simeq 0.1. \tag{8}$$

Equation (8) is used to evaluate N for a given roughness and asperity radius.

RESUSPENSION MODELS

It is well known that the near-wall turbulent flow is dominated by vortical coherent structures and occasional bursts. The state of understanding of near-wall flows were

summarized by Hinze.[33] The near-wall flow behavior is expected to have a profound effect on the particle detachment process. In this section, two models for particle re-entrainment in turbulent flows that are based on wall coherent vortices and burst/inrush phenomena are described.

Sublayer Model

Experimental data and direct numerical simulation have shown that coherent vortices form near the wall and that they persist for long durations in terms of wall unit of time, ν/u^*.[2] Here ν is the kinematic viscosity, $u^* = \sqrt{\tau_w/\rho}$ is the shear velocity, τ_w is the wall shear stress and ρ is the fluid density. The spacing between the vortices is about 100 wall units (of length), ν/u^*. The velocity field in the down-flow region of the coherent vortices was modeled as plan stagnation point flow by Fichman *et al.*[34] and Fan and Ahmadi.[35] Accordingly, the nondimensional velocity components are given as

$$u^+ = y^+, \quad w^+ = 2\beta_0 y^+ z^+, \quad \text{for} \quad y^+ \leqslant 1.85 \tag{9}$$

where $\beta_0 = 0.01085$ and the dimensionless quantities are defined as

$$u^+ = u/u^*, \quad w^+ = w/u^*, \quad y^+ = yu^*/\nu, \quad z^+ = zu^*/\nu. \tag{10}$$

Here, u and w are the fluid velocity in the streamwise and spanwise direction, respectively. Additional details of the sublayer model were described by Fan and Ahmadi.[35]

Equation (10) shows that the maximum transverse velocity occurs at $z^+ = \pm\Lambda^+/4$, where Λ^+ is the streak spacing ($\Lambda \simeq 100$). That is, $w^+|_{\max} = 0.5425y^+$. This implies that the transverse velocity of the coherent near-wall eddies could reach about 50 percent of streamwise velocity. Therefore, their effects must be included in the analysis of particle removal from surfaces.

Figure 1 shows the schematic diagram of a rough surface in contact with a flat plane. In this figure, H_0 denotes the position of the equilibrium separation for which the asperity adhesion force balances the elastic rebound force, k_r is the average roughness height, and e is the distance corresponding to the displaced origin of the velocity profile. Browne[36] provided several expressions for k_r and e as related to the statistical properties of asperities. For small surface roughnesses, those expressions may be approximated as

$$k_r = 5.9\sigma, \quad e = 0.53k_r, \tag{11}$$

where σ is the standard deviation of asperity height.

For surfaces with a small roughness, it is assumed that the near-wall velocities do not change except for the shift in the velocity origin. For a sphere attached to a rough surface using equation (9), the nondimensional velocity components at its centroid are given by

$$u^+ = \frac{d^+}{2} + 2.76\sigma^+ + H_0^+ - \alpha^+, \tag{12}$$

$$w^+ = \beta\frac{\Lambda^+}{2} + \left(\frac{d^+}{2}2.76\sigma^+ + H_0^+ - \alpha^+\right), \tag{13}$$

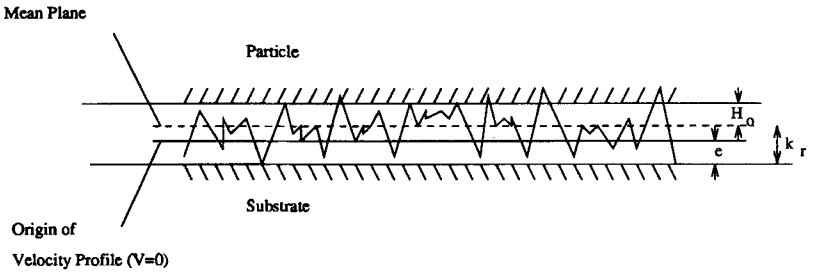

FIGURE 1 Contact of a rough deformable surface with a rigid smooth surface.

where d is the particle diameter, and α is the relative approach between the particle and surface (at the equilibrium condition).

The analytical expressions for the Stokes drag force, the Saffman lift force, and the hydrodynamic couple acting on an attached particle are, respectively, given by

$$F_t = \frac{5.8\pi\rho d u^{*2} L}{C}, \tag{14}$$

$$F_L = \frac{1.95\rho d^2 u^{*3} L}{\nu}, \tag{15}$$

$$M_t = \frac{2.14\pi\rho u^{*2} d^2 L}{C}, \tag{16}$$

where L is defined as

$$L = \frac{d}{2} + 2.76\sigma + H_0 - \alpha. \tag{17}$$

Here the wall correction factors for the hydrodynamic drag and couple as given by O'Neill[37] are included. In equations (14) and (16) the Cunningham factor, C, is given as (Fuchs[38]; Friedlander[39])

$$C = 1 + Kn[1.257 + 0.4\exp(-1.1/Kn)], \tag{18}$$

where the Knudson number is defined as

$$Kn = \frac{2\lambda}{d}. \tag{19}$$

Here λ is the mean free path of air.

Turbulence Burst/Inrush Model

Flow structure during a turbulence burst/inrush was described by Hinze[33] and Johnson and Alfredsson.[40] Cleaver and Yates[15] and Soltani and Ahmadi[23] discussed the turbulence burst/inrush model for particle detachment from smooth surfaces. It was postulated that the flow near the wall during the inrush after the

burst behaves as an axisymmetric viscous stagnation point flow. Accordingly, the maximum velocity in the streamwise flow direction was estimated as

$$u^+ = 1.72y^+ + 0.1y^{+2} \tag{20}$$

Using equation (20) and the model for rough walls described in the previous section, the maximum velocity in the streamwise direction at the level of the particle centroid is given by

$$u^+ = \frac{u^*L}{\nu}\left(1.72 + \frac{0.1u^*L}{\nu}\right). \tag{21}$$

Therefore, the maxima of the drag force, the Saffman lift force, and the hydrodynamic couple acting on an attached particle are, respectively, given as

$$F_t = \frac{5.8\pi\rho d u^{*2} L}{C}\left(1.72 + \frac{0.1u^*L}{\nu}\right), \tag{22}$$

$$F_L = \frac{1.95\rho d^2 u^{*3} L}{\nu}\left(1.72 + \frac{0.1u^*L}{\nu}\right)\left(1.72 + \frac{0.2u^*L}{\nu}\right)^{1/2}, \tag{23}$$

$$M_t = \frac{2.14\pi\rho d^2 u^{*2} L}{C}\left(1.72 + \frac{0.1u^*L}{\nu}\right). \tag{24}$$

PARTICLE DETACHMENT

Figure 2 shows the geometric features of a spherical particle which is attached to a rough surface. A particle will be removed when the external forces overcome the adhesion force. Here, based on the two resuspension models described earlier, the critical shear velocities using the moment and sliding detachment mechanisms are evaluated.

Sublayer-Rolling

Consider a particle which is attached to a rough surface as shown in Figure 2. Applying the angular momentum balance about point "O", the critical force ratio for the onset of rolling detachment becomes

$$\frac{F_t}{F_M} = \frac{a}{\frac{M_t}{F_t} + L + a\frac{F_L - mg}{F_t}}, \tag{25}$$

where m is the mass of the particle, and g is the acceleration of gravity. Substituting equations (4) and (14)–(16) into (25), the critical shear velocity needed to detach the particle from the rough surface becomes

$$u_c^* = \left[\frac{aC[\pi a^2 N f_{po} \exp[-0.6/(\Delta_c)^2] + mg]}{\rho L d^2 (5.04\pi + 1.95\frac{aCu_c^*}{\nu})}\right]^{1/2} \tag{26}$$

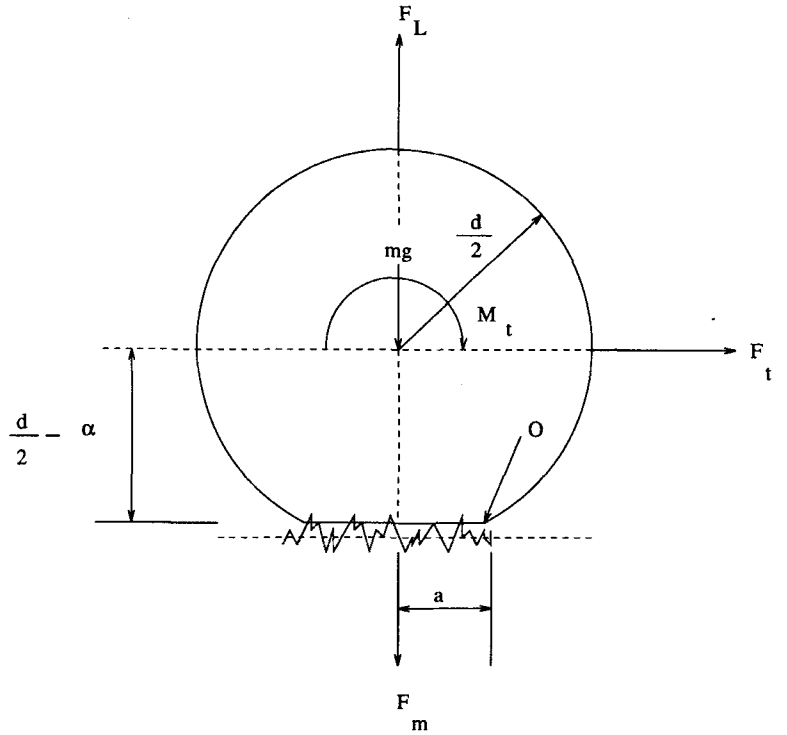

FIGURE 2 Geometric features of a spherical particle attached to a rough surface.

where

$$a = \frac{\pi N f_{po} d}{2K} \exp[-0.6/(\Delta_c)^2]. \tag{27}$$

Note that the critical shear velocity given by equation (26) is sufficient to dislodge the particle and initiate its rolling. While rolling on the surface, should the particle reach a region with a lower level shear velocity, in principle it could re-attach to the wall. However, during the rolling small fluctuations in the flow and/or the lift force could detach the particle. Here we assume that the particles which have begun to roll will be removed from the surface and the possibility of their re-attachment is ignored.

Sublayer-Sliding

According to the sliding detachment model, the particle starts to slide when the external forces equates the friction force, *i.e.*,

$$F_t = k(F_M + mg - F_L), \tag{28}$$

where F_t is the external force (*i.e.*, the fluid drag) acting on the particle in the direction parallel to the surface, and k is the static coefficient of friction. Substituting equations (14) and (15) into (28), the critical shear velocity for sliding detachment

becomes

$$u_c^* = \left[\frac{kC[\pi a^2 N f_{po} \exp[-0.6/(\Delta_c)^2 + mg]}{\rho L d(5.8\pi + 1.95\frac{kCdu_c^*}{\nu})}\right]^{1/2} \tag{29}$$

As in the rolling detachment case, the probability of re-attachment for the sliding particle is also ignored.

Burst-Rolling

For the burst resuspension model, substituting equations (4) and (22)–(24) into (25), the critical shear velocity for rolling detachment becomes

$$u_c^* = \left[\frac{aC(\pi a^2 N f_{po} \exp[-0.6/(\Delta_c)^2] + mg)}{\rho L d^2(1.72 + 0.1\frac{u_c^* L}{\nu})(5.04\pi + 1.95\frac{aCu^*}{\nu}(1.72 + 0.2\frac{u^* L}{\nu})^{1/2}}\right]^{1/2} \tag{30}$$

Burst-Sliding

Substituting equations (4), (22) and (23) into (28), the critical shear velocity for sliding detachment is given as

$$u_c^* = \left[\frac{kC[\pi a^2 N f_{po} \exp[-0.6/(\Delta_c)^2] + mg]}{\rho d L(1.72 + 0.1\frac{u_c^* L}{\nu})(5.8\pi + 1.95\frac{kCdu^*}{\nu}(1.72 + 0.2\frac{u_c^* L}{\nu})^{1/2})}\right]^{1/2} \tag{31}$$

In most practical cases σ, α and H_0 are negligibly small in comparison with $d/2$. Therefore, in equations (26) and (29)–(31), $L \simeq d/2$. In the subsequent analysis the effects of α and H_0 are neglected, but the influence of σ is included.

RESULTS

Figures 3 and 4 compare the critical shear velocities for rubber and graphite particles for different values of Δ_c as predicted by the rolling detachment mechanism. The corresponding material properties are listed in Table I. It is assumed that the radius of asperities varies linearly with particle diameter (*i.e.*, $\beta = 0.02d$), and the contribution of gravity is neglected. Equation (7) was also used for evaluating the surface number density of asperities, N. The results for the smooth surface are also shown in these figures for comparison. It is observed that the critical shear velocity needed to detach a particle increases rapidly as particle diameter decreases. For a specific particle size, Figures 3 and 4 show that the critical shear velocity decreases as the value of Δ_c de- creases (roughness σ/δ_c increases). The critical shear velocity has the highest value for the smooth surface and becomes quite small for highly rough surfaces with $\Delta_c = 0.4$.

For the conditions of Figures 3 and 4, the simulations were repeated with the Saffman lift force being neglected. It was found that the predicted critical shear velocities essentially did not change. This observation shows that the effect of lift force on particle resuspension is negligible.

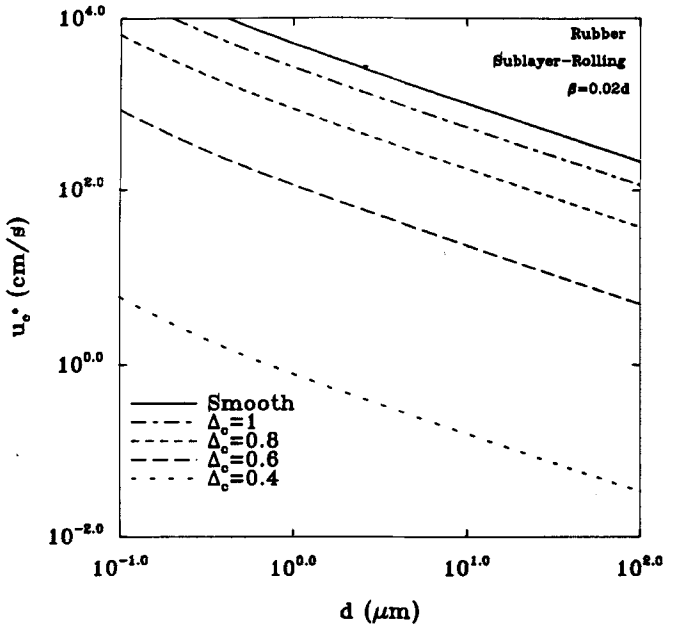

FIGURE 3 Variations of the critical shear velocity with particle diameter for different values of Δ_c for rubber particles.

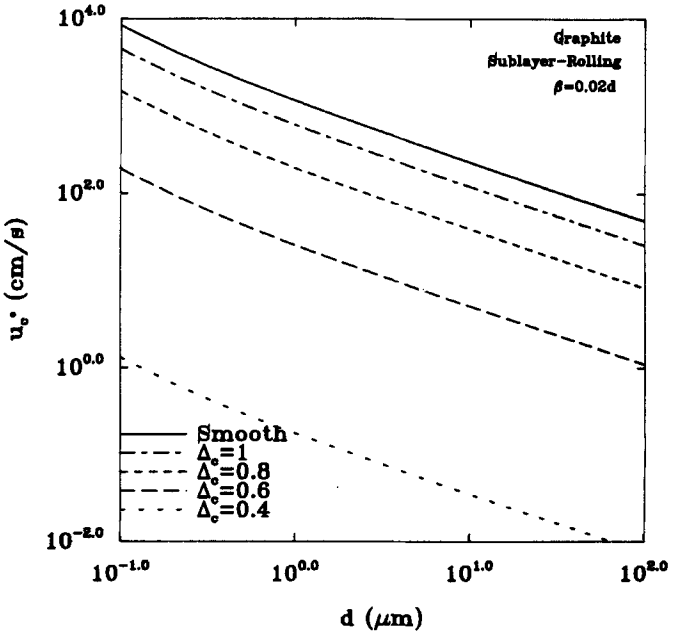

FIGURE 4 Variations of the critical shear velocity with particle diameter for different values of Δ_c for graphite, particles.

TABLE I
Material Properties

Material	E (10^8 dyn/cm^2)	A (10^{-13} ergs)	W_A (ergs/cm^2)	ν_i	ρ (g/cm^3)	k	Ref.
Rubber	0.24	20.5	34	0.5	1.13	0.8	9
Graphite	67500	46.9	77.75	0.16	2.2	0.1	13
Glass (Dry air)	6900	8.5	14.1	0.2	2.18	0.9	13
Glass (Moist air)	6900	320	530	0.2	2.18	0.9	43
Steel	21500	21.2	35	0.28	7.84	0.58	13
Glass-Steel	—	—	150	—	—	0.6	30

Comparison of Figures 3 and 4 shows that the critical shear velocity for rubber is larger than that for graphite for both smooth and rough surfaces. This trend occurs in spite of the fact that the surface energy of rubber is less than half of W_A for graphite. The main reason is that the modulus of elasticity for graphite is 10^5 times as large as that for rubber. It then follows that the contact radius for a rubber sphere is about 65 times as large as that for a graphite sphere. Thus, the corresponding adhesion moment resistance is reduced proportionately.

Figure 5 shows the variation of the critcal shear velocity with asperity radius for 10 μm rubber particles in accordance with the rolling detachment mechanism for different values of Δ_c. It is observed that the critical shear velocity decreases with

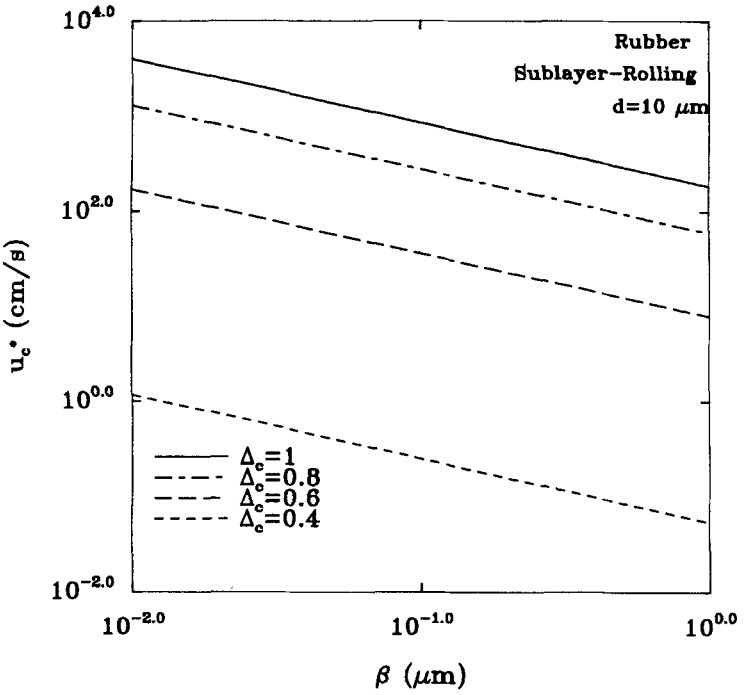

FIGURE 5 Variations of the critical shear velocity with aspirity radius for different values of Δ_c.

increasing asperity radius for all values of Δ_c. Note also that as β increases, equation (8) implies that the number of asperities decreases which further reduces the net adhesion force.

Variation of the critical shear velocity with the surface roughness (standard deviation of asperity height, σ) for 50 μm rubber particles in accordance with the rolling detachment mechanism is shown in Figure 6. Here, the value of $\beta = 2.5$ μm is used. It is observed that the critical shear velocity decreases rapidly as the roughness (σ) increases. As was mentioned before, for real surfaces the quantities N, β, and σ are related by equation (8). Therefore, $N \simeq 0.04/\sigma$ and, consequently, the trend of variation of the critical shear velocity with the number density of asperities can also be seen from Figure 6.

Effects of surface roughness on particle removal according to various detachment mechanisms and different resuspension models are shown in Figures 7 and 8. Here, the values of $\Delta_c = 0.6$, $\beta = 0.02d$ and the coefficients of friction of 0.8 and 0.1, respectively, for rubber and graphite are used. It is observed that the particles are removed from rough surfaces at much lower velocities when compared with those for smooth surfaces. For example, a critical shear velocity of about 10 m/s is needed to resuspend a 10 μm rubber particle from a smooth surface based on the sublayer model by the rolling mode. However, for the rough surface, the corresponding shear velocity is about 0.1 m/s. Figures 7 and 8 show that the burst model leads to critical

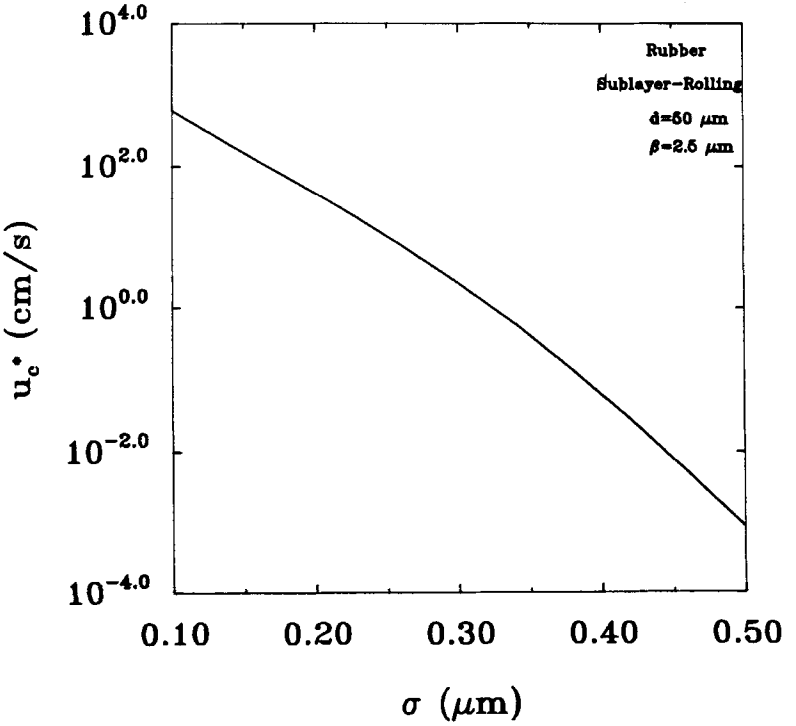

FIGURE 6 Variations of the critical shear velocity with surface roughness.

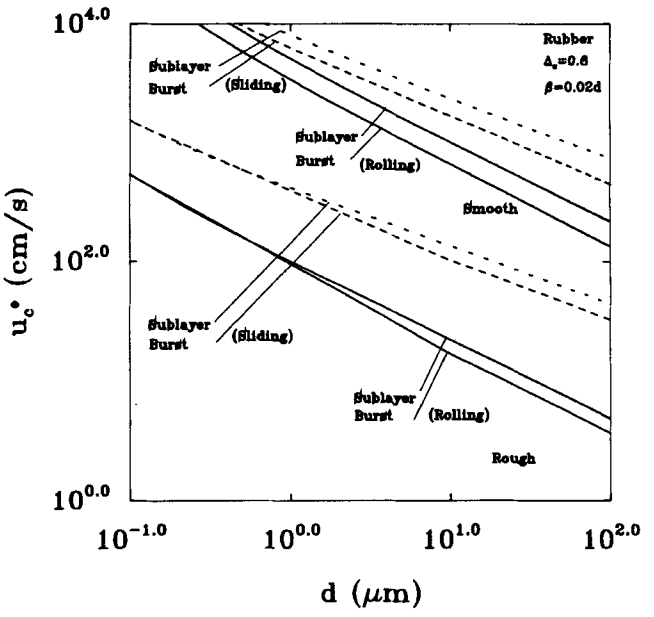

FIGURE 7 Comparison of critical shear velocities for smooth and rough surfaces for rubber particles in accordance with various detachment mechanisms and different resuspension models.

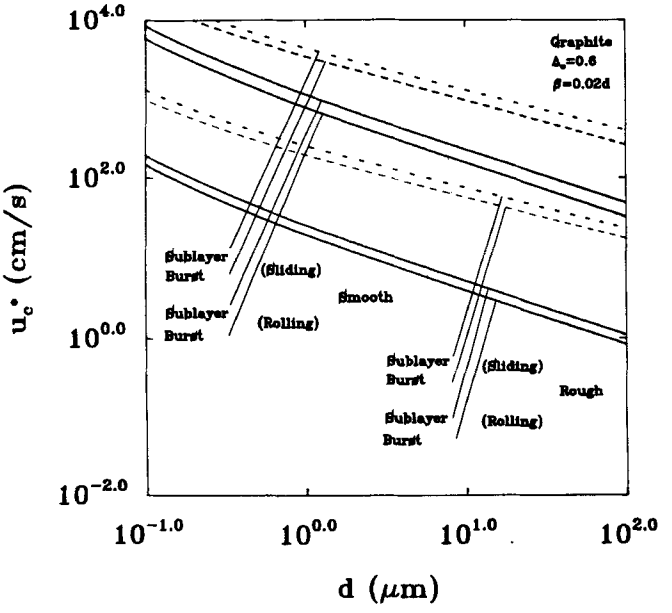

FIGURE 8 Comparison of critical shear velocities for smooth and rough surfaces for graphite particles in accordance with various detachment mechanisms and different resuspension models.

shear velocities for particle resuspension which are lower than those predicted by the sublayer model. It is also observed that the particle rolling detachment occurs at much lower u_c^* when compared with the particle sliding detachment.

Figure 9 compares the critical shear velocity for rubber particles in accordance with various detachment mechanisms for different values of asperity radius. It is observed that the critical shear velocity increases as the asperity radius decreases. Similiar to Figure 7, the rolling detachment requires the minimum critical shear velocity for particle detachment.

To study the effect of gravity and its direction on the critical shear velocity, a series of numerical simulations was performed. The results (not shown here due to space limitation) show that the effect of gravity is, generally, negligible, except for small values of Δ_c (large roughnesses) and large particles.

COMPARISON WITH EXPERIMENTAL DATA

In this section the model predictions are compared with the experimental data of Taheri and Bragg[41] and Zimon[42] for resuspension of particles. The experiment of Taheri and Bragg was carried out, using a Preston tube to determine the effect of free stream velocity, shear velocity, and shear stress on resuspension of glass

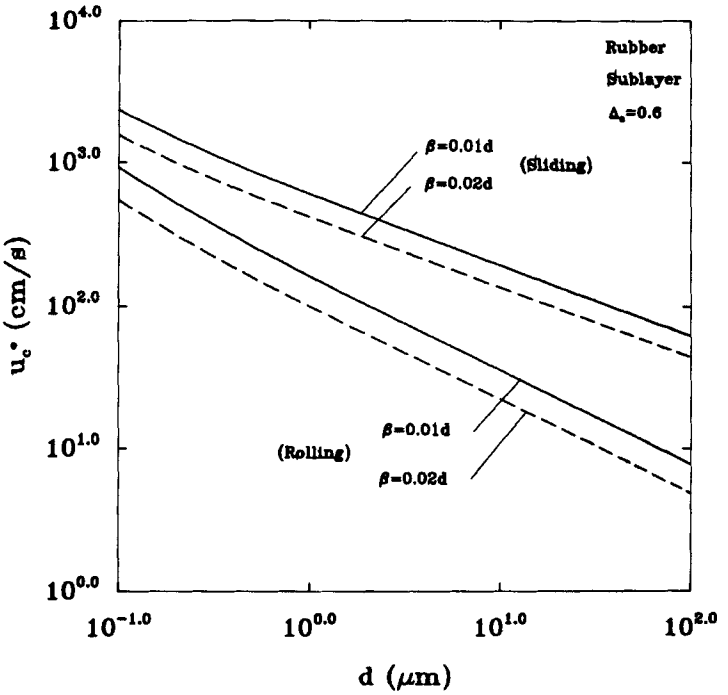

FIGURE 9 Comparison of critical shear velocities for various detachment mechanisms and different asperity radii.

particles from a glass surface. The range of free stream velocities was from 2 to 130 m/s. The experimental data of Zimon[42] was for entrainment of glass particles which were lying on a steel wall. In both experiments particle removal was acheived by air blowing.

Figure 10 and 11 show the variations of critical shear velocities with particle diameter for different values of Δ_c for glass particles in accordance with the rolling and sliding detachment mechanisms as predicted by the sublayer and the burst models, respectively. The corresponding material properties used for glass are listed in Table I. Note that the value of Hamaker constant for the glass in moist air as given by Tomlinson[43] is 320×10^{-13} ergs. Visser[4] however, reported a value of 8.5×10^{-13} ergs for the dry air (or vacuum) condition. It is well-known that the small spaces at the interface of particles and substrates allows for condensation of water vapor to take place at humidities much lower than the saturation condition. That, in turn, would increase the adhesion force significantly. Since the experiment was performed under normal room temperature and humidity conditions, the moist air condition is, generally, assumed. The model predictions for the dry air and smooth surfaces are also shown in Figures 10 and 11. The experimental data of Taheri and Bragg[41] for removal of 20 μm and 35 μm glass particles for various percentages of removal are reproduced in these figures for comparison. It is observed that all the data points are lower than the critical shear velocities for the

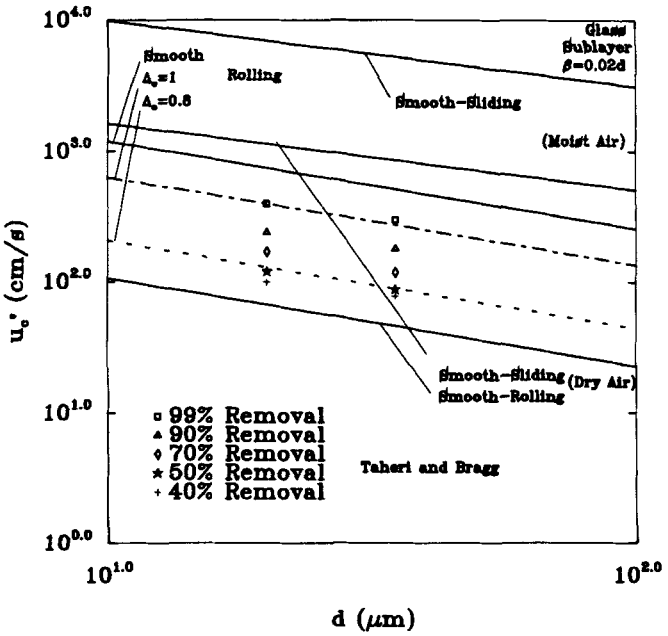

FIGURE 10 Comparison of critical shear velocities as predicted by the sublayer model with the experimental data of Taheri and Bragg[41] for glass particles.

moist air condition, but they are all higher than those for the dry air condition. Therefore, the moist air assumption appears to be reasonable. Figures 10 and 11 also show that the presence of a slight surface roughness reduces the critical shear velocity significantly. It may then be concluded that the scatter in the data is due to the relative humidity of the air, as well as to the presence of small, effective surface roughnesses. These figures also show that the particles are resuspended mainly by the rolling rather than by the sliding mechanism. Earlier, the initial rolling of particles was observed experimentally by Masironi and Fish.[16]

Figures 10 and 11 also show that at lower levels of shear velocity, certain particle removal percentages are achieved. This could be due to the presence of a small roughness. That is, depending on the way that the particles are placed on the surface, individual particles may experience different small roughness (of the order of atomic scales) in regard to their effective adhesion force. Thus, some particles could be removed at shear velocities lower than that required for detachment under a completely smooth surface condition.

It should be pointed out that the model predictions for the dry air (vacuum) condition and the sliding detachment model including the roughness effects are also in qualitative agreement with the experimental data. However, since the experiment was not done under the vacuum condition, such agreement may be only fortuitous.

Figure 12 shows the variation of the critical shear velocity as a function of particle diameter for detaching glass particles from a steel substrate in accordance with the

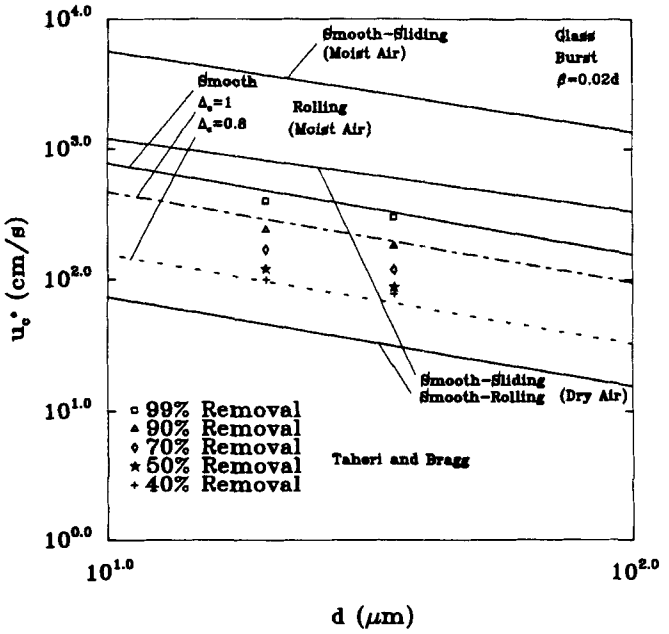

FIGURE 11 Comparison of critical shear velocities as predicted by the burst model with the experimental data of Taheri and Bragg[41] for glass particles.

rolling detachment mechanism as predicted by the sublayer and burst models. The corresponding material properties used for the glass-steel interface are listed in Table I. Experimental data of Zimon[42] for removal of glass particles from a steel surface are also reproduced in this figure for comparison. Since Zimon only reported the critical free stream detaching velocities, the corresponding shear velocities were estimated using $u^* \simeq 0.04\,U$. The critical detaching velocity was obtained by Zimon using the assumption of a log-normal distribution of the adhesion force. Figure 12 shows that the experimental data are in good agreement with the model prediction for $\Delta_c = 0.9$. This value of Δ_c corresponds to roughnesses of $\sigma = 2\,\text{Å}$ and $8\,\text{Å}$ for particle diameters $d = 10$ and $100\,\mu\text{m}$, respectively. For seemingly smooth surfaces, such small values of roughness may be expected to be present.

Figure 13 shows the variation of u_c^* with particle diameter for entrainment of glass particles from a steel surface. Experimental data of Zimon[42] are also shown in this figure for comparison. It is observed that the predicted critical shear velocities for sliding removal are much higher than those for rolling detachment. The experimental data of Zimon[42] agree with the model prediction result for a roughness of $\Delta_c = 0.55$ ($\sigma/\delta_c \simeq 1.8$). This value of roughness is about 1.6 times that for the rolling detachment case (with $\Delta_c = 0.9$) shown in Figure 12.

Figures 12 and 13 show that particle removal from rough surfaces could be achieved by both a rolling and a sliding mechanism. Spherical particles, however,

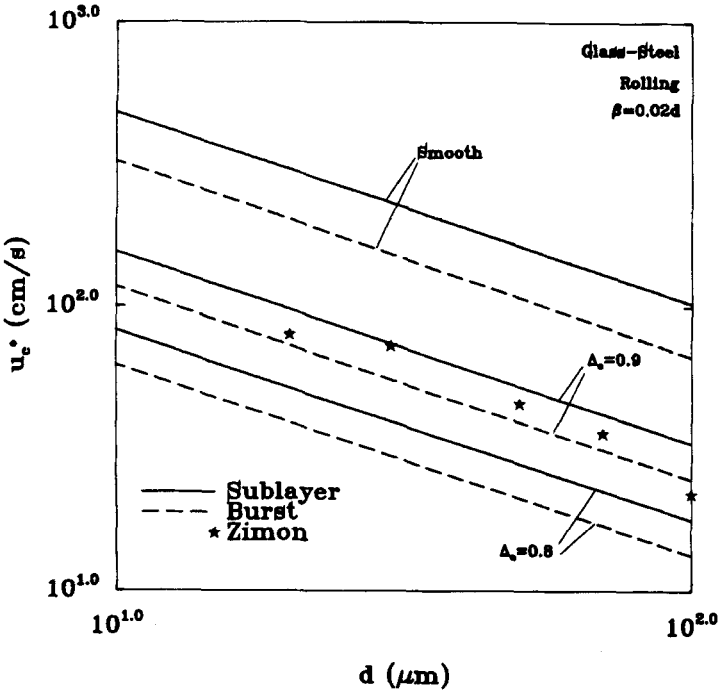

FIGURE 12 Comparison of critical shear velocities as predicted by the rolling model with the experimental data of Zimon[42] for glass particles removal from a steel substrate.

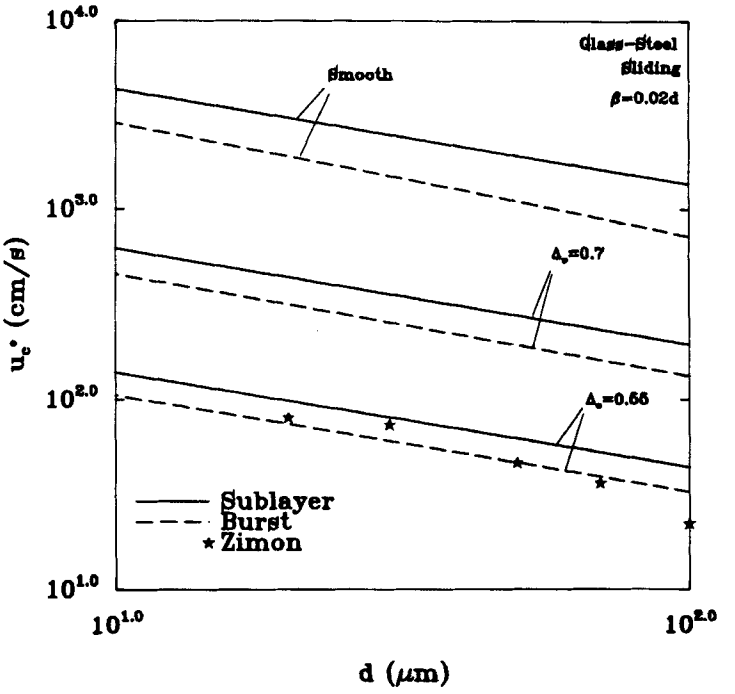

FIGURE 13 Comparison of critical shear velocities as predicted by the sliding model with the experimental data of Zimon[42] for glass particles removal from a steel substrate.

are more easily dislodged by the rolling motion in comparison with the sliding mechanism.

CONCLUSIONS

Particle resuspensions from rough surfaces based on the sublayer and turbulence burst/inrush models using the theory of rolling and sliding removal are studied. General expressions for the critical shear velocities required to detach a particle from a rough surface are derived. Based on the presented results, the following conclusions may be drawn:

1. The rolling detachment is the dominant resuspension mechanism for spherical particles on rough surfaces.
2. The critical shear velocity reduces sharply as roughness increases.
3. The critical shear velocity increases as the radius of asperities decreases.
4. The effect of gravity on particle resuspension is negligible. Such effects may become noticeable as surface roughness and/or particle size increases.
5. The effect of the Saffman lift force on particle resuspension for smooth and rough surfaces is negligible.

6. The sublayer vortical motion and the turbulence burst/inrush are important for removal of particles from rough as well as smooth surfaces.
7. For hard elastic materials (with a high elastic modulus), small surface roughnesses (of the other of atomic scale) could reduce the critical shear velocity significantly.
8. The model predictions for rolling detachment are in reasonable agreement with the experimental data for glass particle detachment from glass and steel substrates.
9. Critical shear velocities predicted by the sliding detachment agree with the experimental data only if relatively high values of surface roughness are assumed.

The presented results are for spherical particles and surface roughnesses which are much smaller than the particle size. The effect of particle geometries and surface roughnesses larger than the particle size are not included in this study.

Acknowledgements

Thanks are given to Mr. Michael A. Gaynes and Mr. Raymond G. Bayer of IBM-Endicott for their many helpful suggestions and comments. Various stages of this work was supported by International Business Machines (IBM-Endicott), the New York State Science and Technology Foundation through the Center for Advanced Material Processing (CAMP) of Clarkson University, and the US Department of Energy (University Coal Research Program, PETC), under Grant DE-FG22-94 PC 94213.

References

1. M. Corn, in *Aerosol Science*, C. N. Davies, Ed. (Academic Press, New York, 1966), p. 359.
2. A. D. Zimon, *Adhesion of Dust and Powder*. (Plenum Press, New York, 1969), 1st ed.
3. H. Krupp, *Adv Colloid Interface Sci.* **1**, 111–140 (1967).
4. J. Visser, in *Surface and Colloid Science*, E. Matijevic, Ed. (Plenum Press, New York, 1976) **8**, pp. 3–84.
5. D. Tabor, *J. Colloid Interface Sci.* **58**, 2–13 (1977).
6. R. A. Bowling, *J. Electrochem. Soc. Solid State Science Technol.* **132**, 2208–2219 (1985).
7. M. B. Ranade, *J. Aerosol Sci. Technol.* **7**, 161–176 (1987).
8. B. V. Derjaguin, *Koll. Zhur.* **69**, 155–164 (1934).
9. K. L. Johnson, K. Kendall and A. D. Roberts, *Proc. Royal. Soc. Lond.* **324**, 301–313 (1971).
10. B. V. Derjaguin, V. M. Muller and Y. P. T. Toporov, *J. Colloid Interface Sci.* **53**, 314–326 (1975).
11. V. M. Muller, V. S. Yushenko and B. V. Derjaguin, *J. Colloid Interface Sci.* **77**, 91–101 (1980).
12. V. M. Muller, V. S. Yushenko and B. V. Derjaguin, *J. Colloid Interface Sci.* **92**, 92–101 (1983).
13. C. J. Tsai, D. Y. H. Pui and B. Y. H. Liu, *J. Aerosol Sci. Technol.* **15**, 239–255 (1991).
14. D. S. Rimai, L. P. DeMejo and W. Vreeland, *J. Appl. Phys.* **71**, 2253–2258 (1992).
15. J. W. Cleaver and B. Yates, *J. Colloid Interface Sci.* **44**, 464–474 (1973).
16. L. A. Masironi and B. R. Fish, in *Surface Contamination*, B. R. Fish, Ed., Proc. of a Symposium at Gatlinburg, Tennessee, USA (Pergamon Press, Oxford, 1967), pp. 55–59.
17. J. S. Punjrath and D. R. Heldman, *J. Aerosol Sci.* **3**, 429–440 (1972).
18. J. W. Healy, in *Transuranics in Natural Environments*, M. G. White and P. B. Dunaway, Eds. (USERDA, Las Vegas, 1977), pp. 211–222.
19. G. A. Sehmel, *Environ. Intl.* **4**, 107–127 (1980a).
20. W. J. Smith, F. W. Whicker and H. R. Meyer, *Nuclear Safety*, **23**, 685–699 (1982).
21. W. C. Hinds, *Aerosol Technology, Properties, Behavior, and Measurement of Airborne Particles* (John Wiley and Sons, New York, 1982).
22. K. W. Nicholson, *Atmospheric Environment* **22**, 2639–2651 (1988).

23. M. Soltani and G. Ahmadi, *J. Adhesion Sci. Technol.* **8**, 763–785 (1994).
24. H. Y. Wen and G. Kasper, *J. Aerosol Sci.* **20**, 483–498 (1989).
25. J. A. Greenwood and J. B. P. Williamson, *Proc. Roy. Soc. A.* **295**, 300–319 (1966).
26. J. A. Greenwood, *J. Lub. Tech. Trans. ASME.* **89**, 81–91 (1967).
27. J. A. Greenwood and J. H. Tripp, *J. Appl. Mech.* **67**, 153–159 (1967).
28. K. N. G. Fuller and D.Tabor, *Proc. Roy. Soc. A.* **345**, 327–340 (1975).
29. K. L. Johnson, in *Theoretical and Applied Mechanics*, W. T. Koiter, Ed. (North-Holland, New York, 1976), pp. 133–143.
30. M. W. Reeks, J. Reed and D. Hall, *J. Phys. D: Appl. Phys.* **21**, 574–589 (1988).
31. M. W. Reeks and D. Hall, *J. Fluid Eng.* **110**, 165–171 (1988).
32. M. Soltani and G. Ahmadi, Report No. MAE-270, Clarkson University, (1993). Also *J. Adhesion Sci. Technol.* (In press).
33. J. O. Hinze, *Turbulence* (McGraw-Hill, New York, 1975), 2nd ed.
34. M. Fichman, C. Gutfinger, and D. Pnueli, *J. Aerosol Sci.* **19**, 123–136 (1988).
35. F. G. Fan and G. Ahmadi, *J. Aerosol Sci.* **24**, 45–64 (1993).
36. L. W. B. Browne, *Atmos. Environ.* **8**, 801–816 (1974).
37. M. E. O'Neill, *Chem. Eng. Sci.* **23**, 1293–1298 (1968).
38. N. A. Fuchs, *The Mechanics of Aerosols* (Macmillan, New York, 1964).
39. S. K. Friedlander, *Smoke, Dust and Haze* (John Wiley, New York, 1977).
40. A. V. Johnson and P. H. Alfredsson, *J. Fluid Mech.* **122**, 295–314 (1982).
41. M. Taheri and M. Bragg, *J. Aerosol Sci. Technol.* **16**, 15–20 (1992).
42. A. D. Zimon, *Adhesion of Dust and Powder* (Consultants Bureau, New York, 1982), 2nd ed.
43. G. A. Tomlinson, *Phil. Mag.* **6**, 695 (1928).